some aspects of monsoon research at IAP

Yali Zhu, Institute of Atmospheric Physics
zhuyl@mail.iap.ac.cn

Outline

- **the late 1990s' shift in East China summer rainfall**
- **connection between autumn Arctic sea ice and spring Eurasia soil moisture**
- **Simulation and Projection of Permafrost degradation on the Tibetan Plateau**

1. the late 1990s' shift in East China summer rainfall

Background: changes in East China summer rainfall pattern in the late 1990s

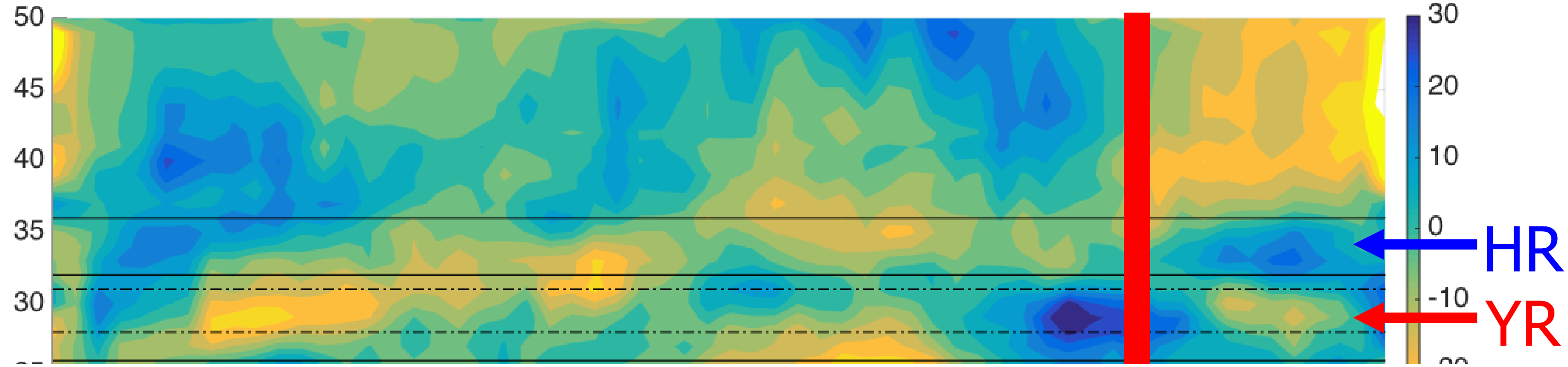

Increased (decreased) summer rainfall over HR (YR) after the late 1990s

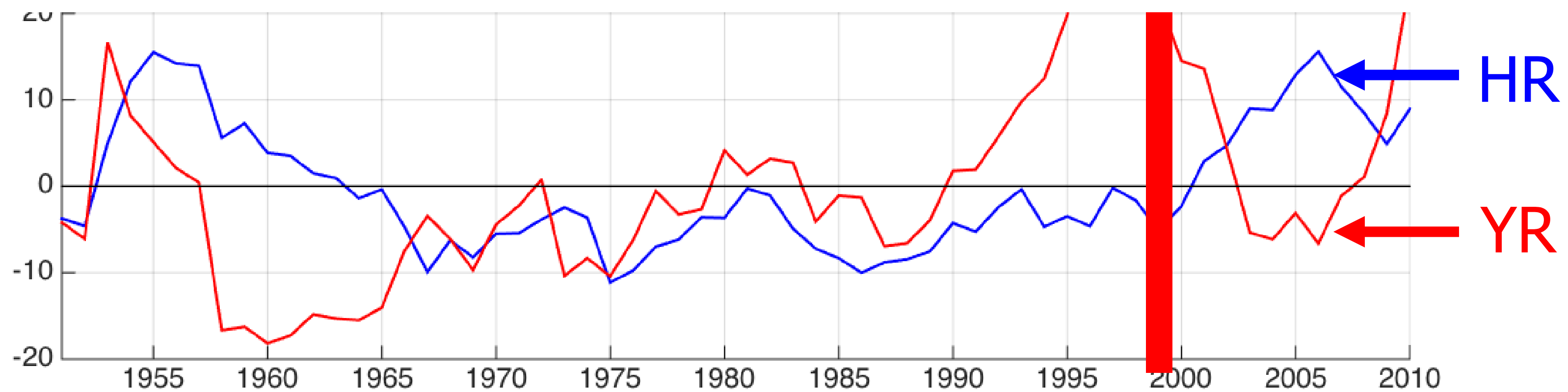

Zhu et al., 2011, CD

SST difference

2000-2010 minus 1979-1998

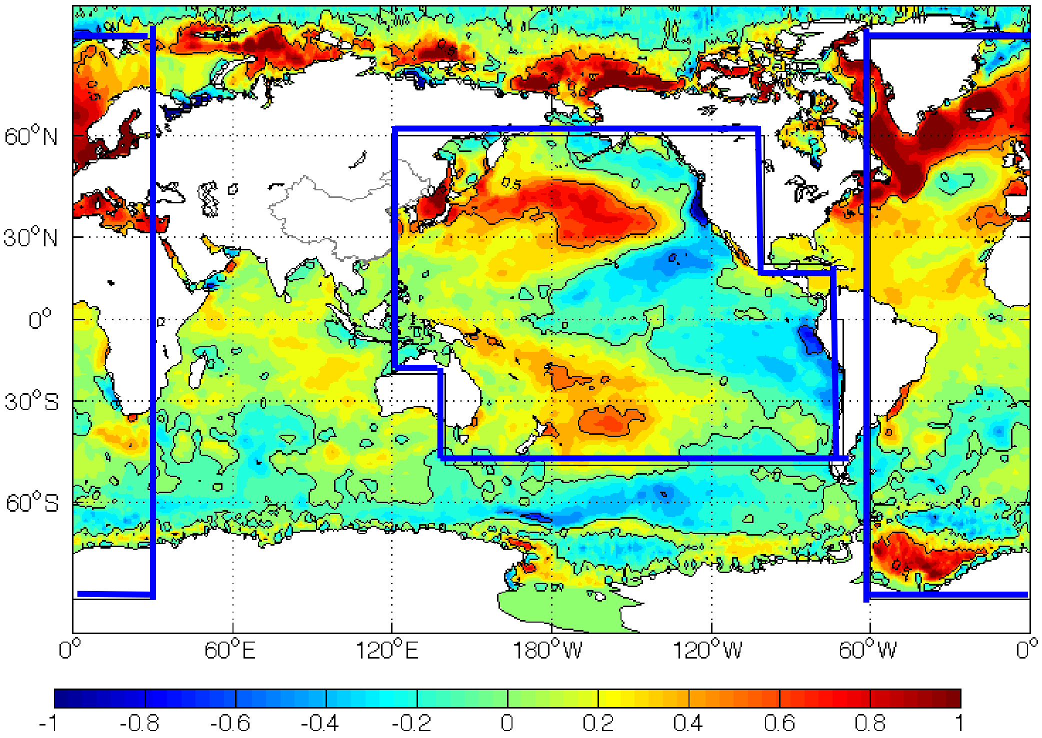

Model: CAM 4
2.5° lat × 1.9° lon

(1) control experiment (Exp_{ctl})

(2) sensitive experiments

(Exp_{Psst}/Exp_{Asst})

- PDO + AMO

Omega & Rainfall

observation | PDO | AMO

omega

rainfall

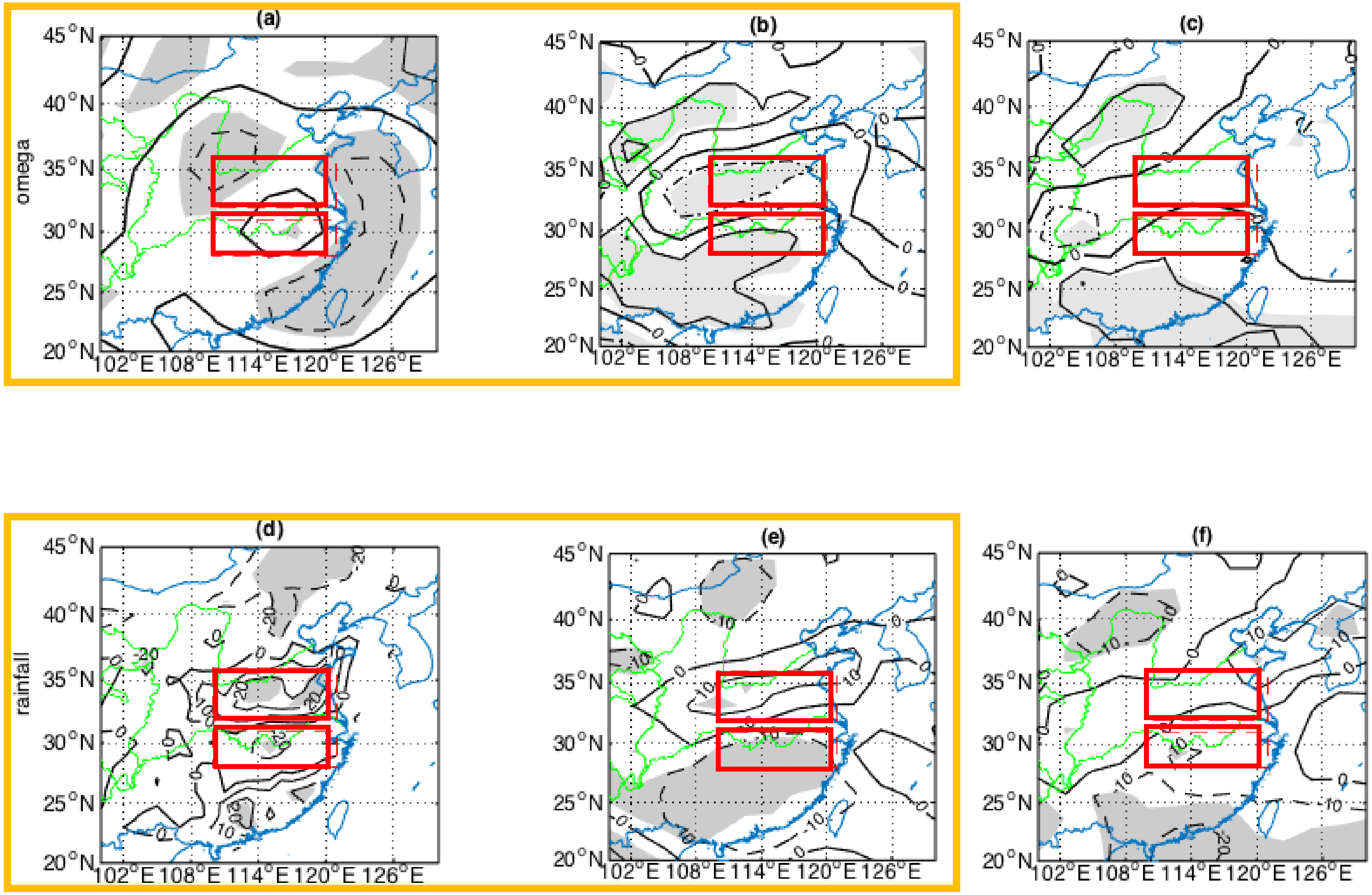

2000-2010
1979-1998

Exp_{Psst} -Exp_{ctl}

Exp_{Asst}-Exp_{ctl}

Zhu et al., 2015, JGR

200 hPa wind: weakened EAWJS

observation

PDO

AMO

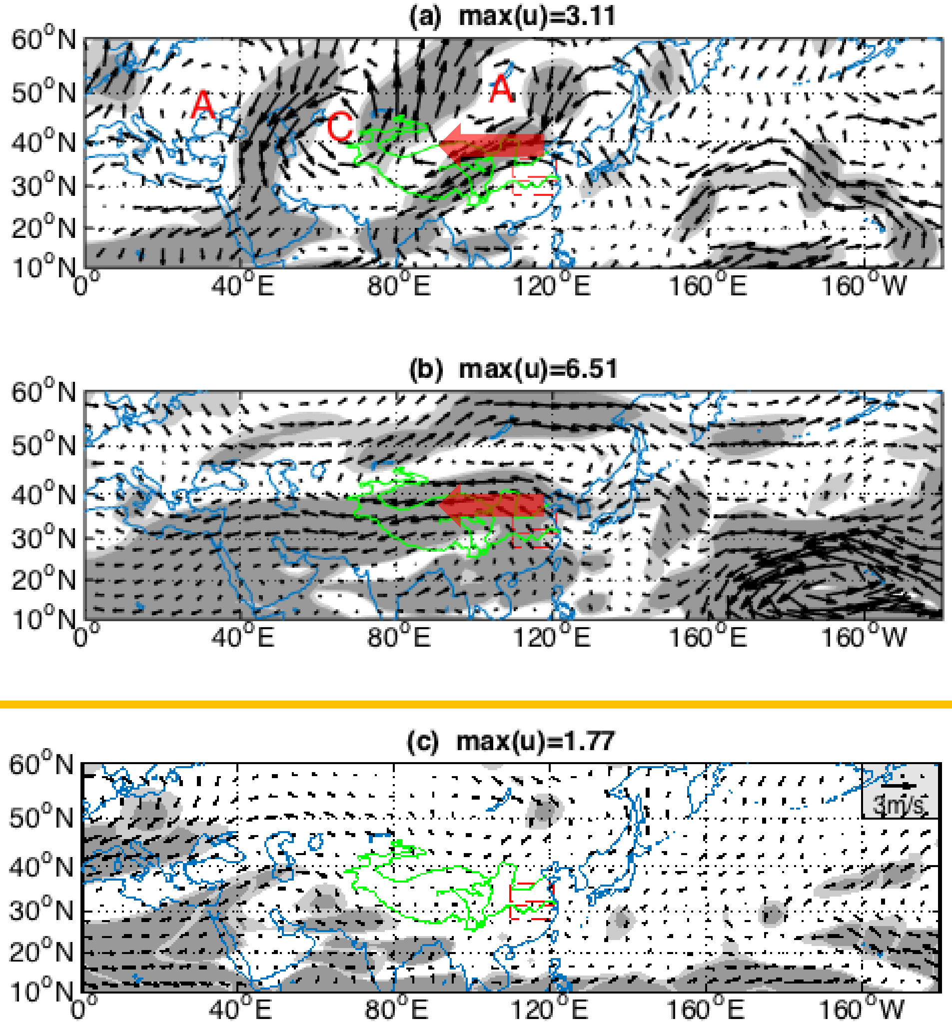

Zonal wind velocity (90°-120°E)

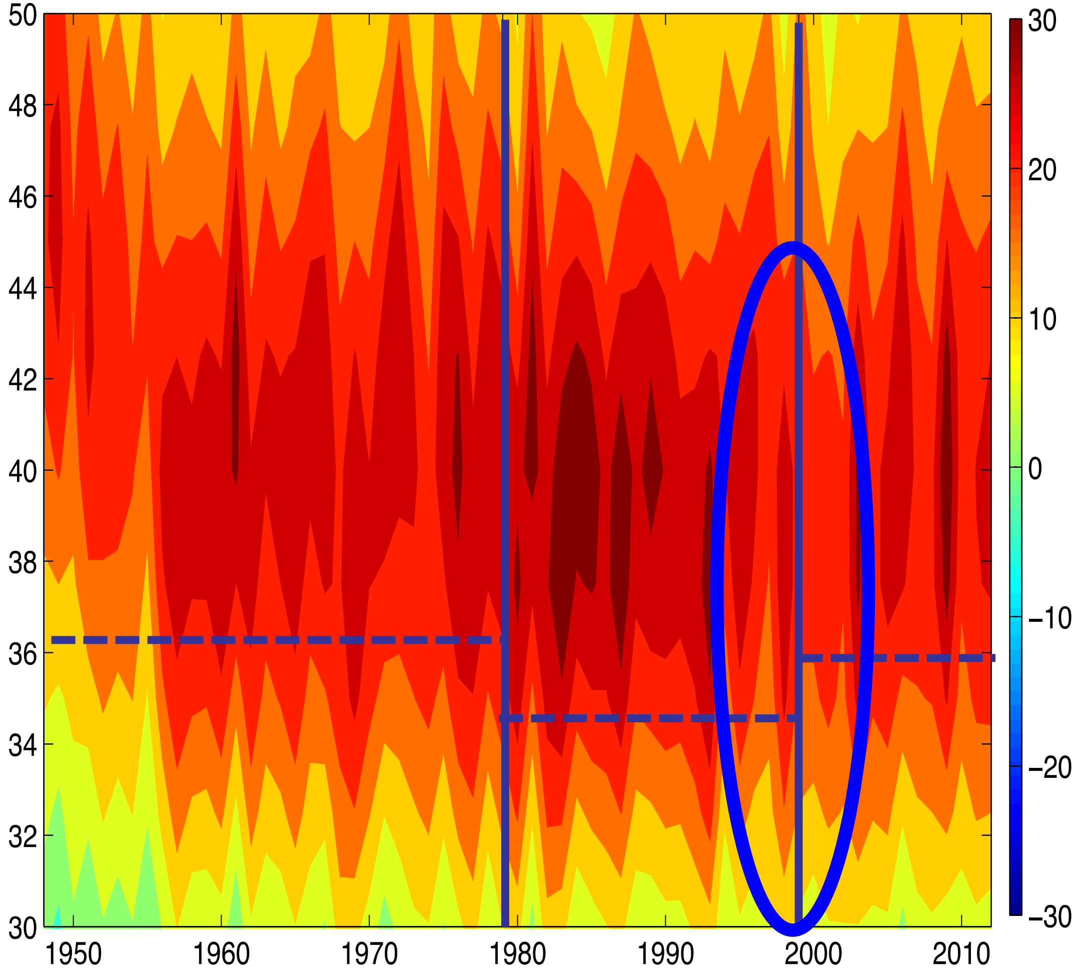

Meridional-vertical wind

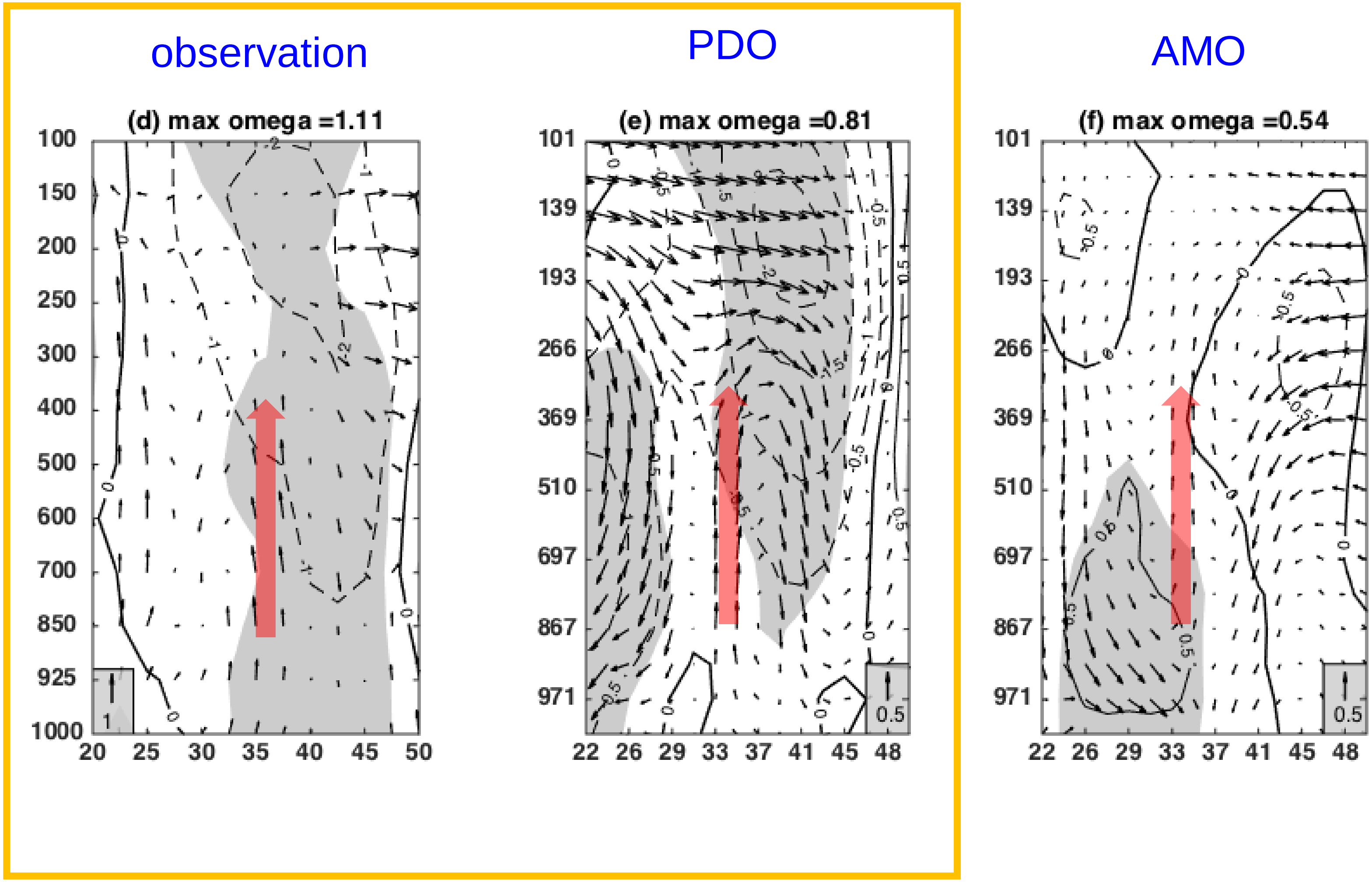

Results from CGCM: CCSM4

Zhu et al., 2016, AAS

- CCSM4：
  - Atmosphere component: 1°, 26 levels
  - Ocean component1°, 60 levels
  - Sea ice and land surface scheme
- 501-year control run
  - Fixed concentration of greenhouse gases and tropospheric aerosol (1850)
- Only internal variability, no long-term trend

Summer precipitation:

+PDO
+AMO

+PDO
–AMO

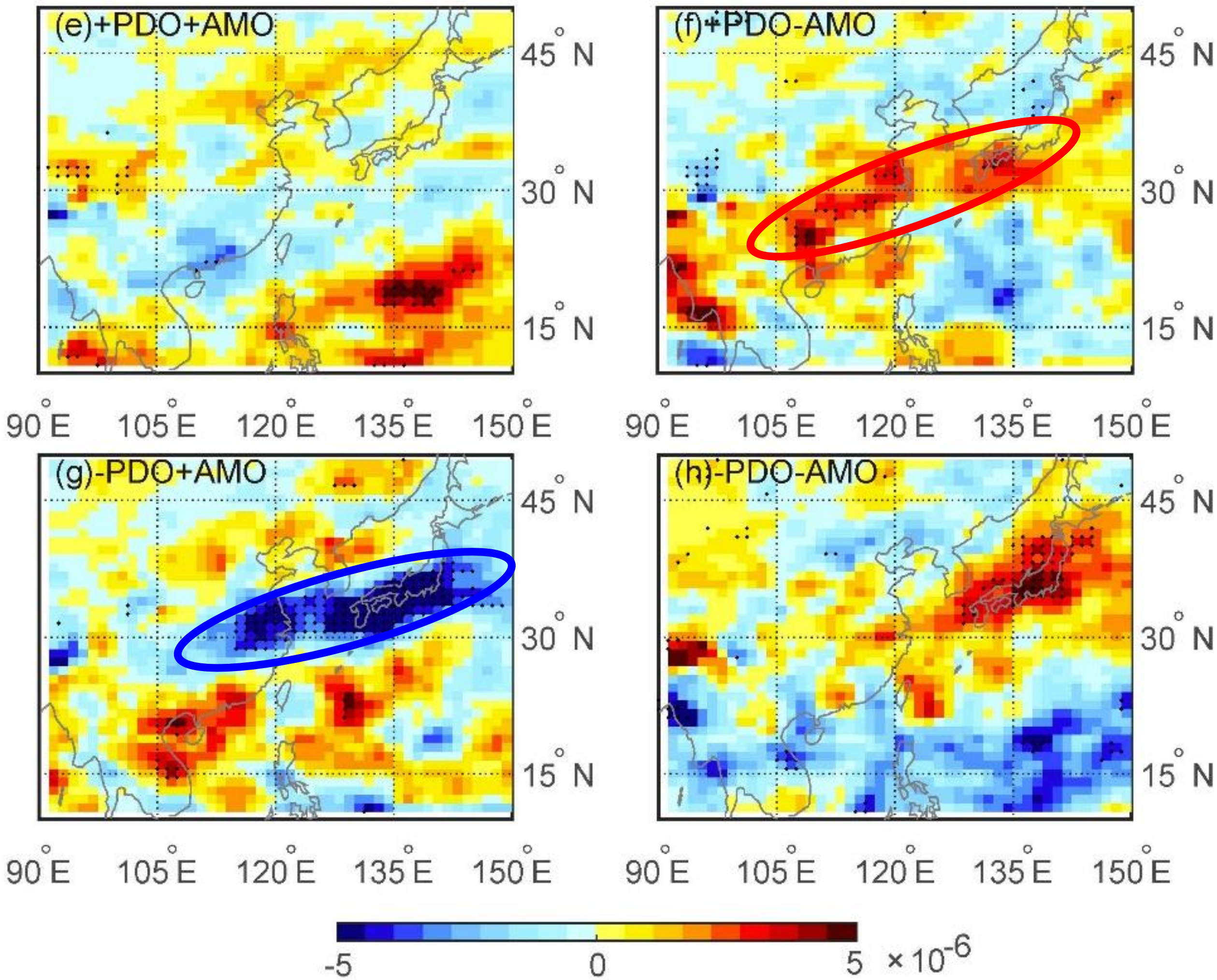

–PDO
+AMO

–PDO
–AMO

200 hPa wind and geopotential height

+PDO
+AMO

+PDO
–AMO

–PDO
+AMO

–PDO
–AMO

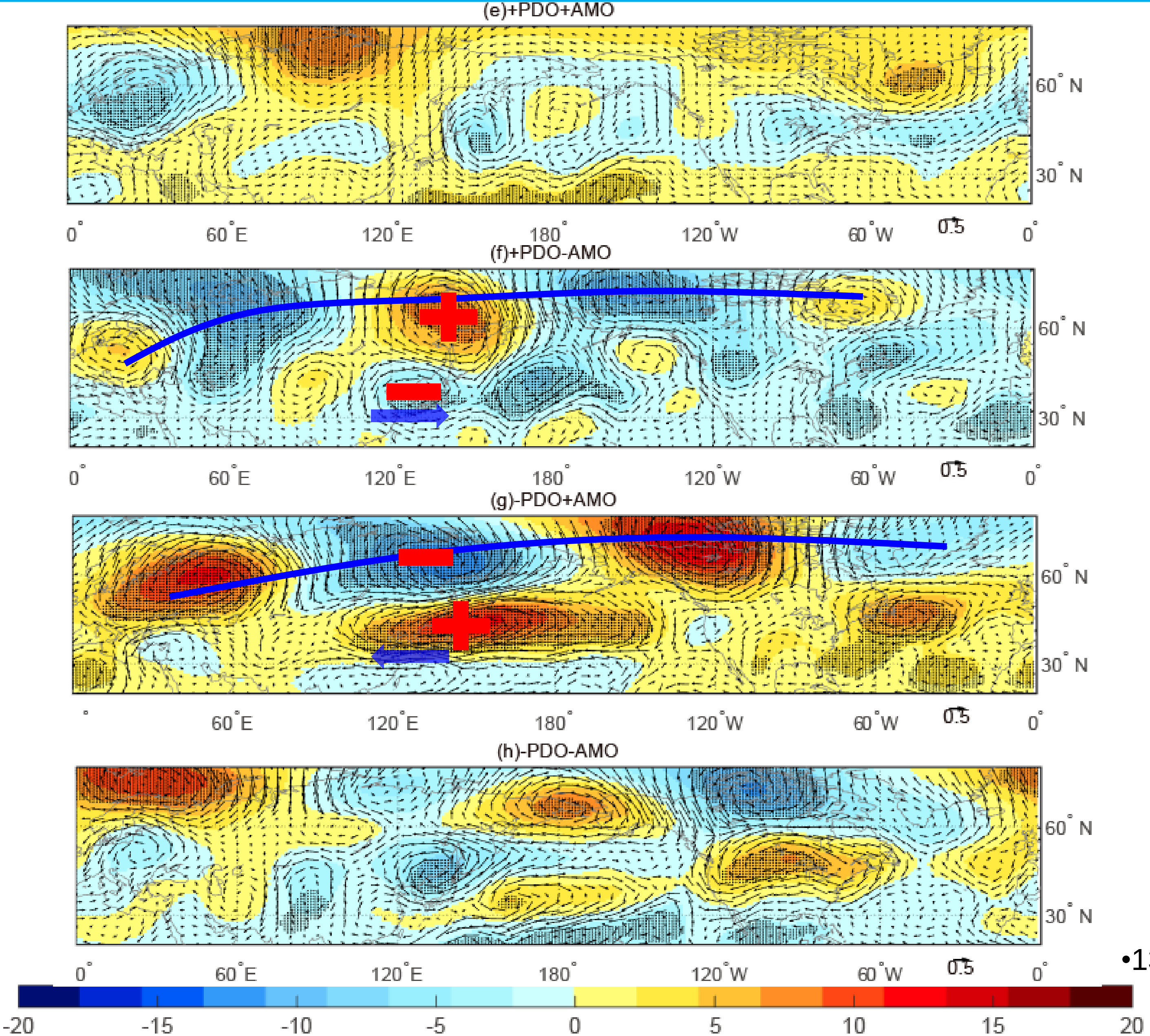

Vertical velocity ω (110°–120°E average)

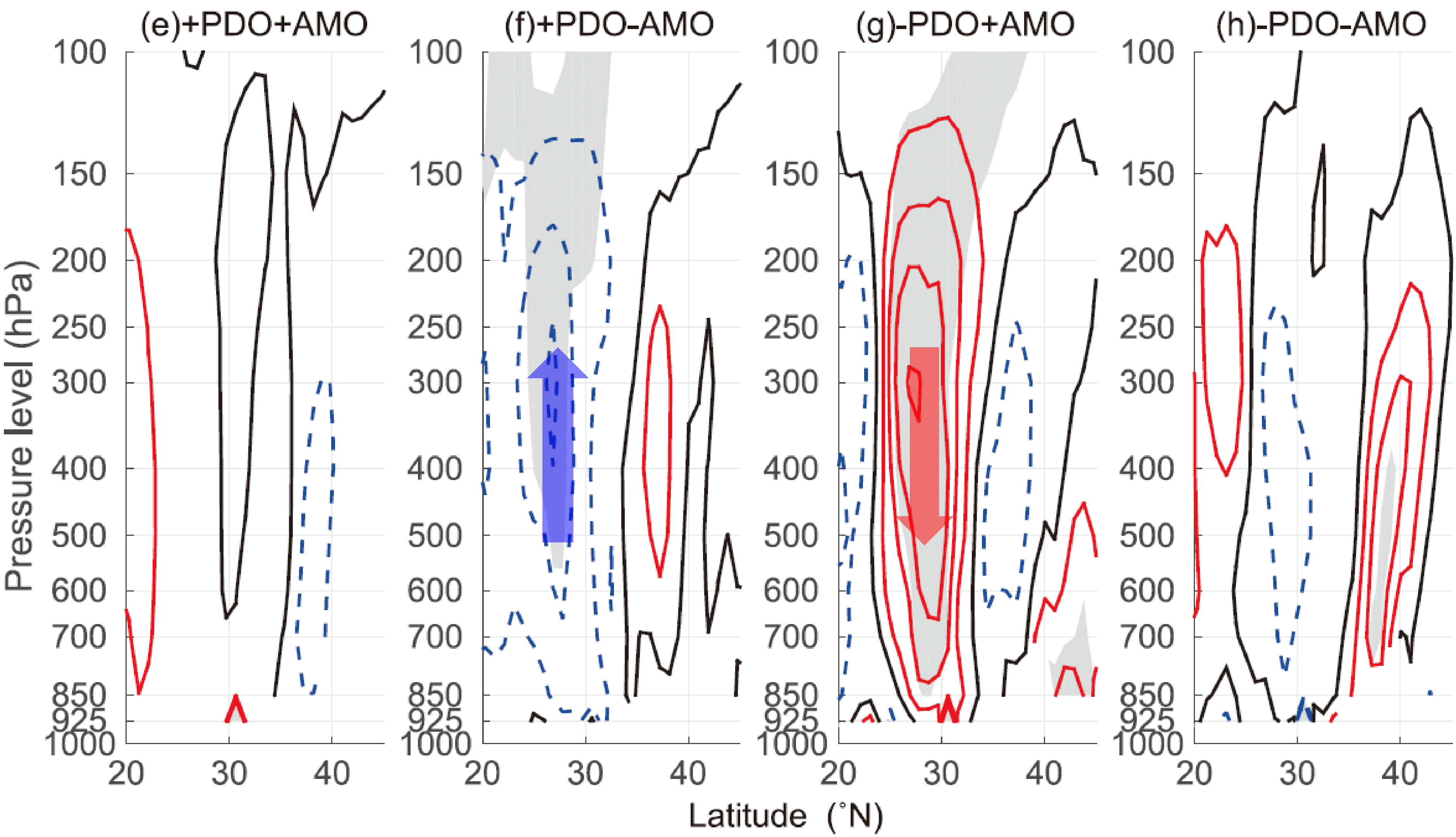

Observation: late 1970s’ and 1990s’ change

PDO/AMO指数

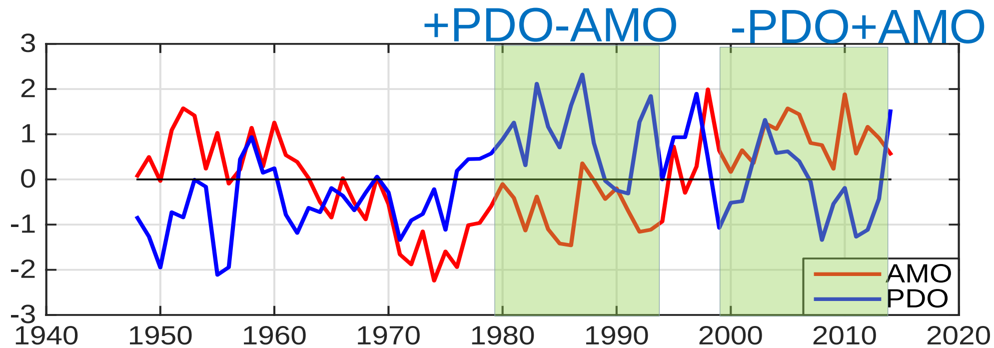

EAWJS
Rainfall

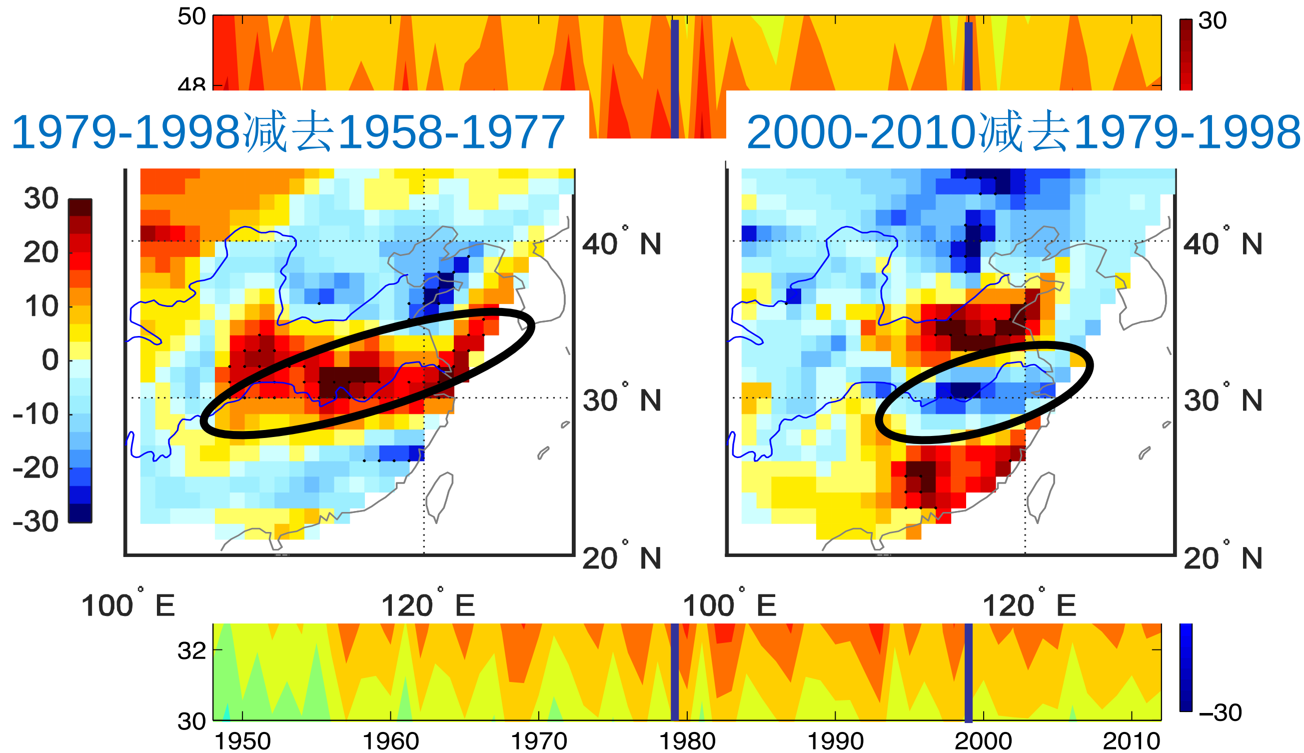

•15

Key Points

- Using AGCM CAM4, PDO can significantly contribute to the summer rainfall changes in East China.
- CGCM results: When the opposite phase of PDO and AMO appear simultaneously, significant anomalous rainfall appear over eastern China. But the relationship between PDO and AMO is not stable.
- EAWJS acts as a bridge in linking the PDO/AMO with summer rainfall in East China through modulating the local meridional-vertical circulation.

Snow depth over the Tibetan Plateau--station data

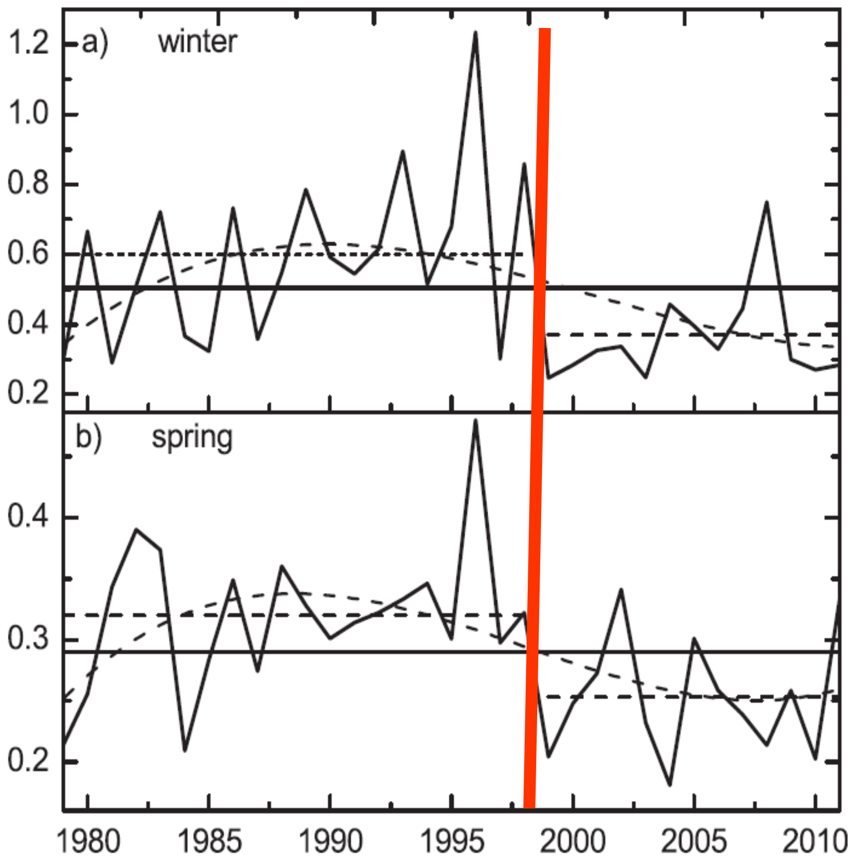

FIG. 2. Time series of (a) winter and (b) spring snow depth (cm day^{-1}) over the Tibetan Plateau, averaged for the 72 stations from 1979 to 2011. The dashed curve indicates the third-order polynomial fit. The horizontal dashed lines indicate averaged values for the two decadal periods 1979–99 and 2000–11. The horizontal solid lines indicate averaged values for the period 1979–2011.

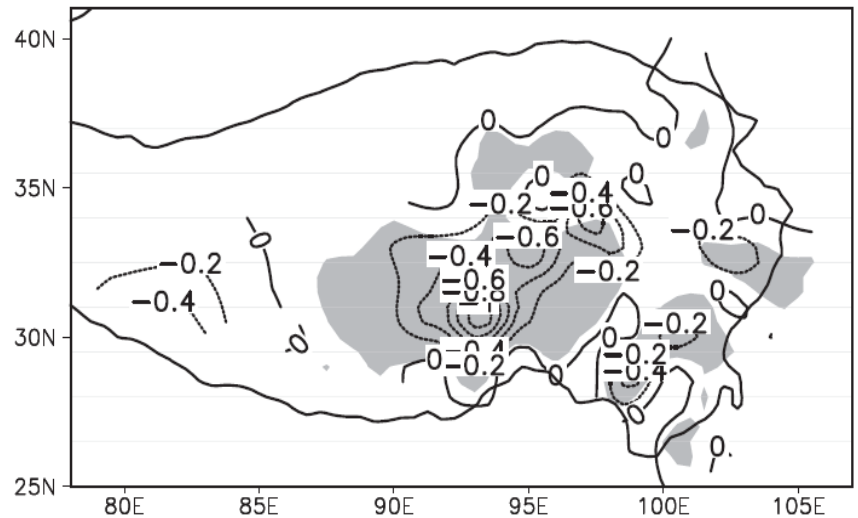

FIG. 3. Changes (2000–11 mean minus 1980–99 mean) in winter snow depth (cm day^{-1}) over the Tibetan Plateau based on the surface-observed data. The shaded areas are statistically significant at the 95% confidence level according to a Student's t test.

From Si and Ding, 2013

- **2. interdecadal change in the connection between Autumn Arctic Sea ice & spring Eurasia soil moiture**

1st SVD mode (1948-2012)

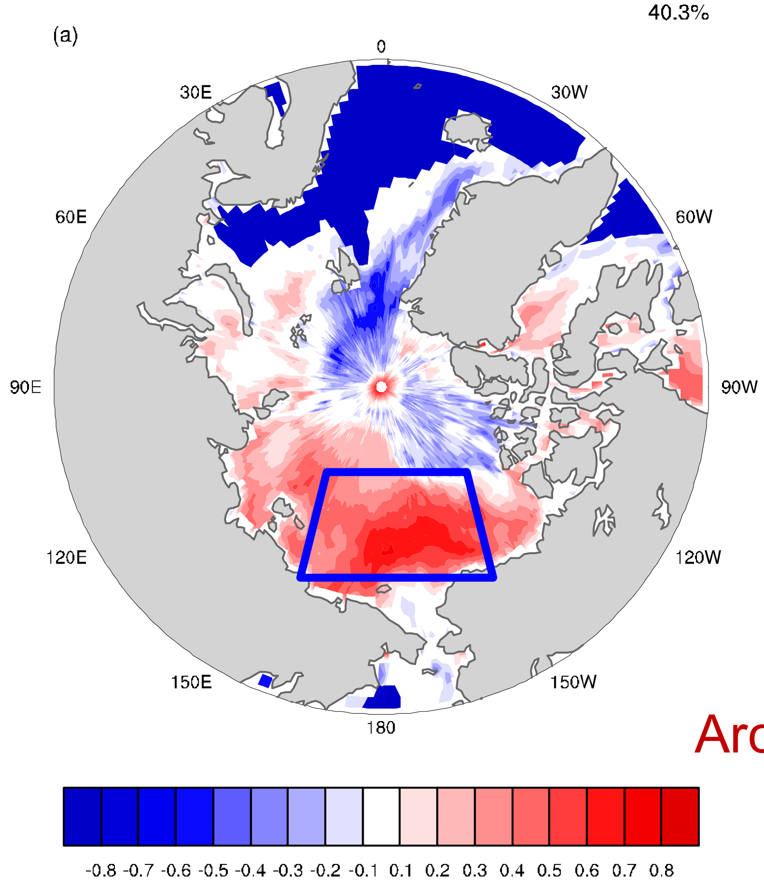

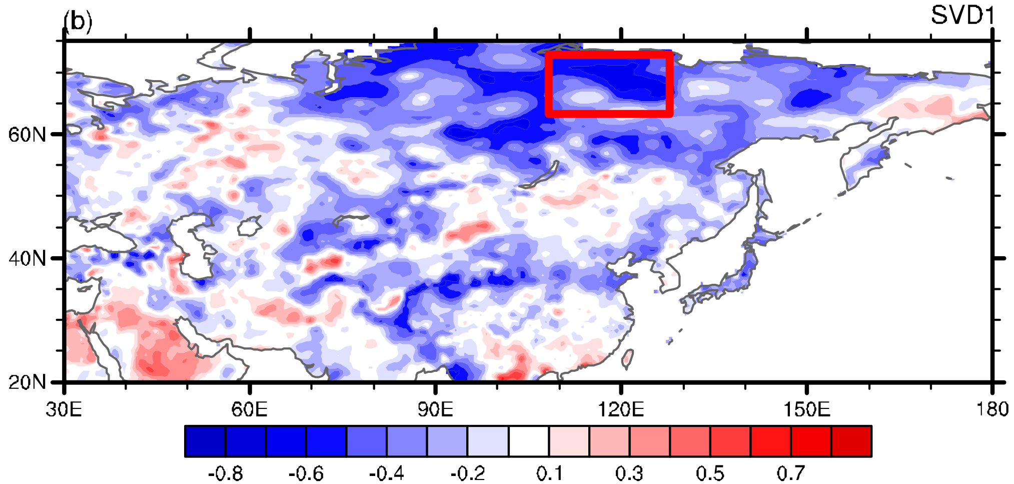

Arctic sea ice index: 150ºE−150ºW, 70º−80ºN;
soil moisture index: 60-70˚N, 110-130˚E

interdecadal change after 1985

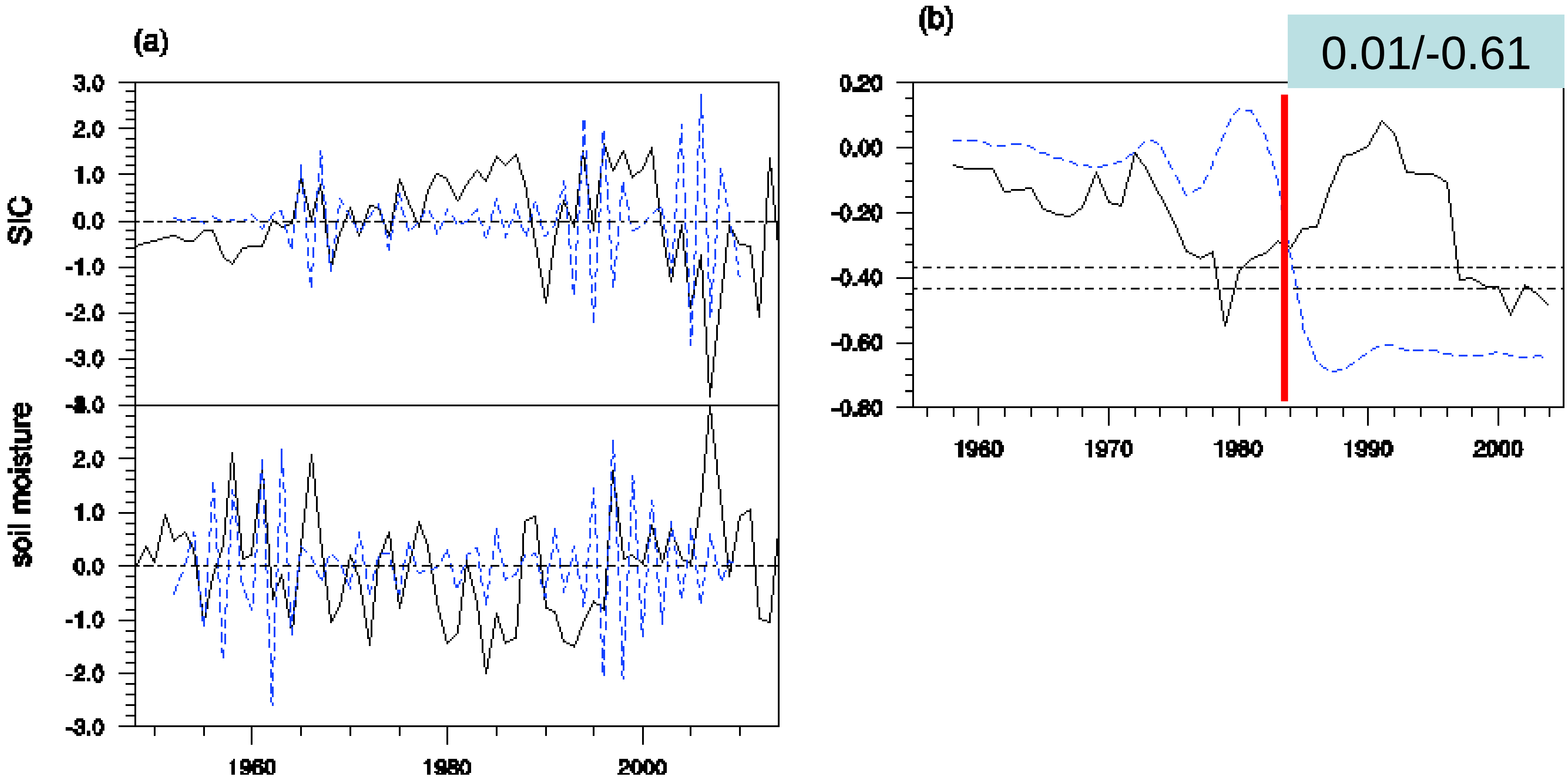

interdecadal change

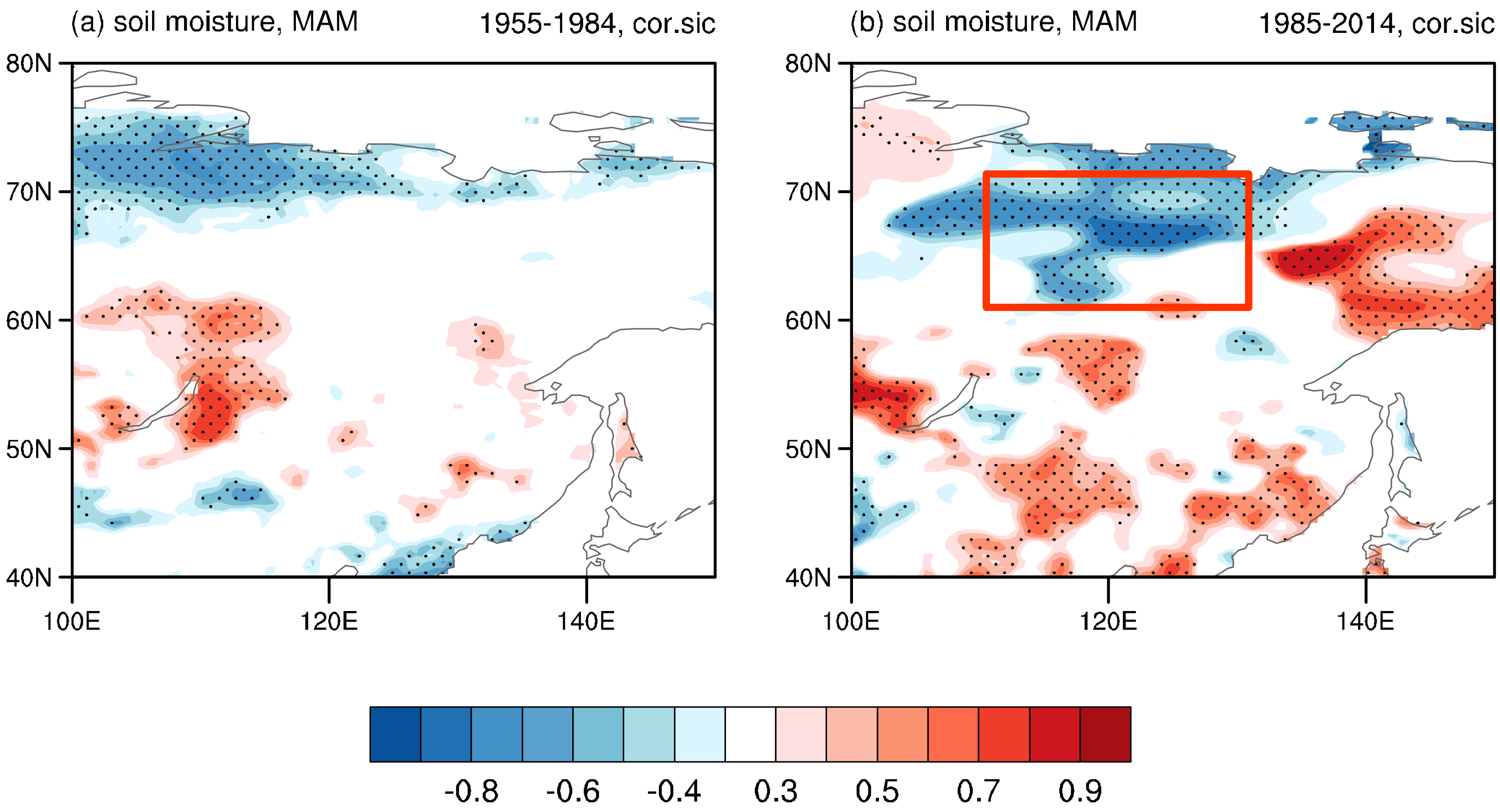

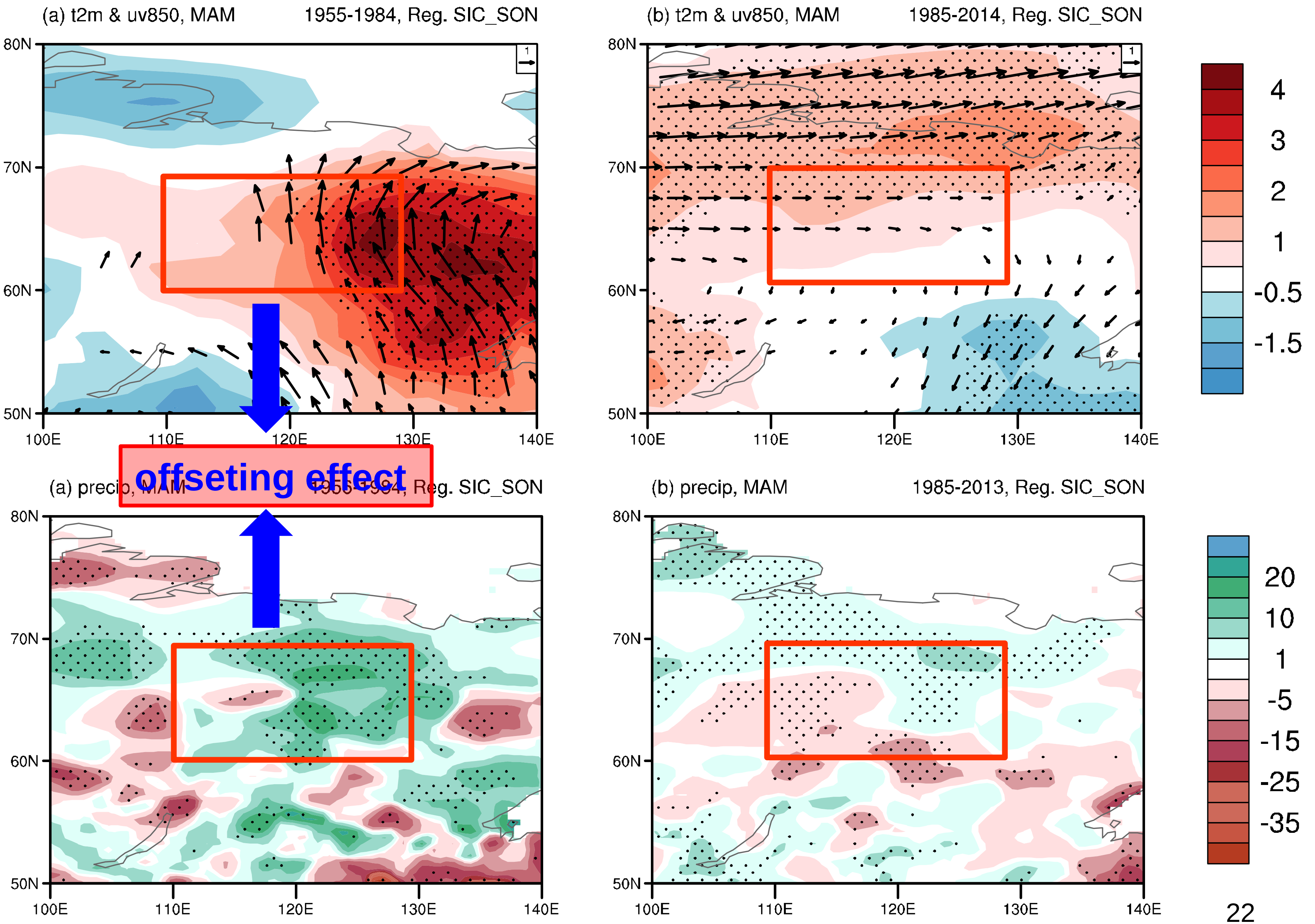
(a) t2m & uv850, MAM
1955-1984, Reg. SIC_SON
(b) t2m & uv850, MAM
1985-2014, Reg. SIC_SON
offseting effect
(a) precip, MAM
1955-1984, Reg. SIC_SON
(b) precip, MAM
1985-2013, Reg. SIC_SON
80N
70N
60N
50N
100E
110E
120E
130E
140E
4
3
2
1
-0.5
-1.5
20
10
1
-5
-15
-25
-35

22

atmospheric circulation & SIC in autumn

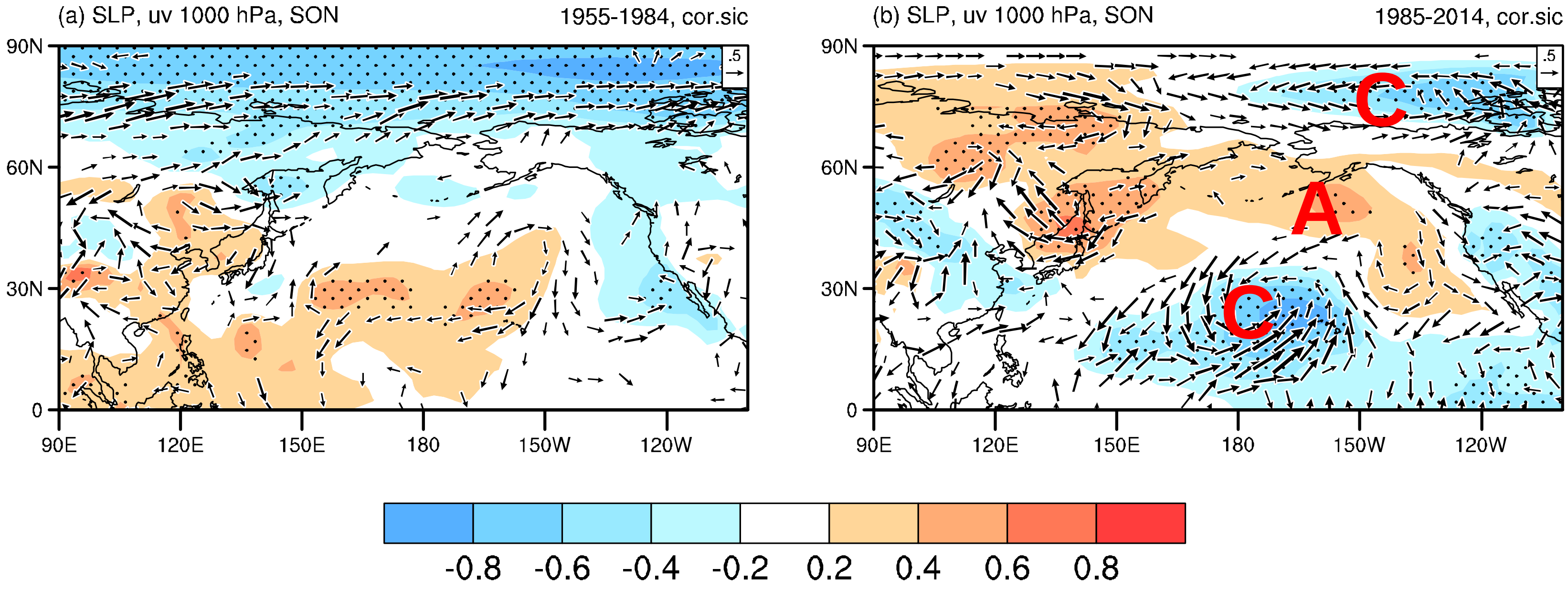

atmospheric circulation & SIC in autumn

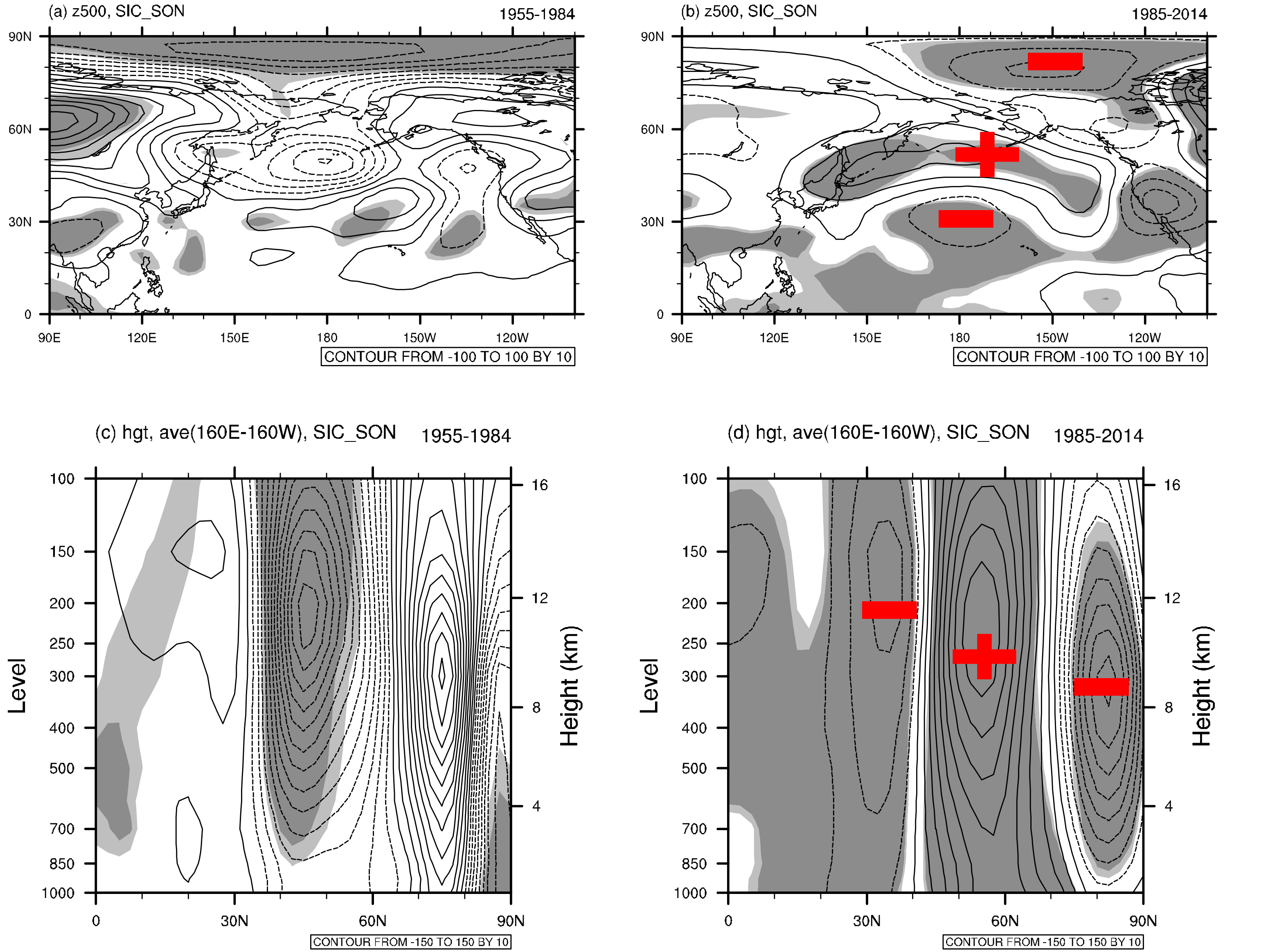

SST

SON

DJF

MAM

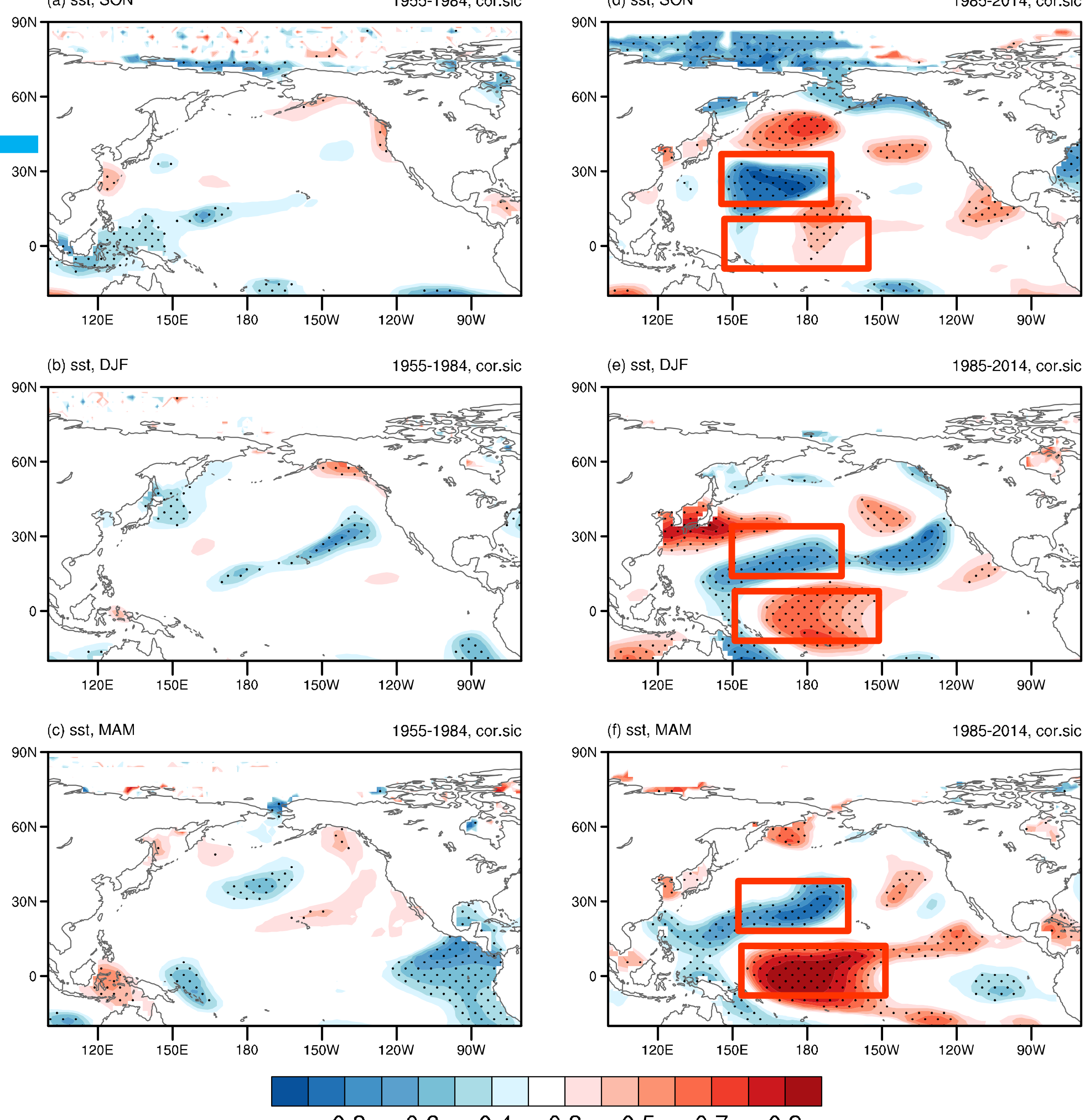

SSTI: difference between 155ºE−155ºW, 10ºS−10ºN and 150ºE−170ºW, 20º−30ºN

correlation with the SSTI after 1985

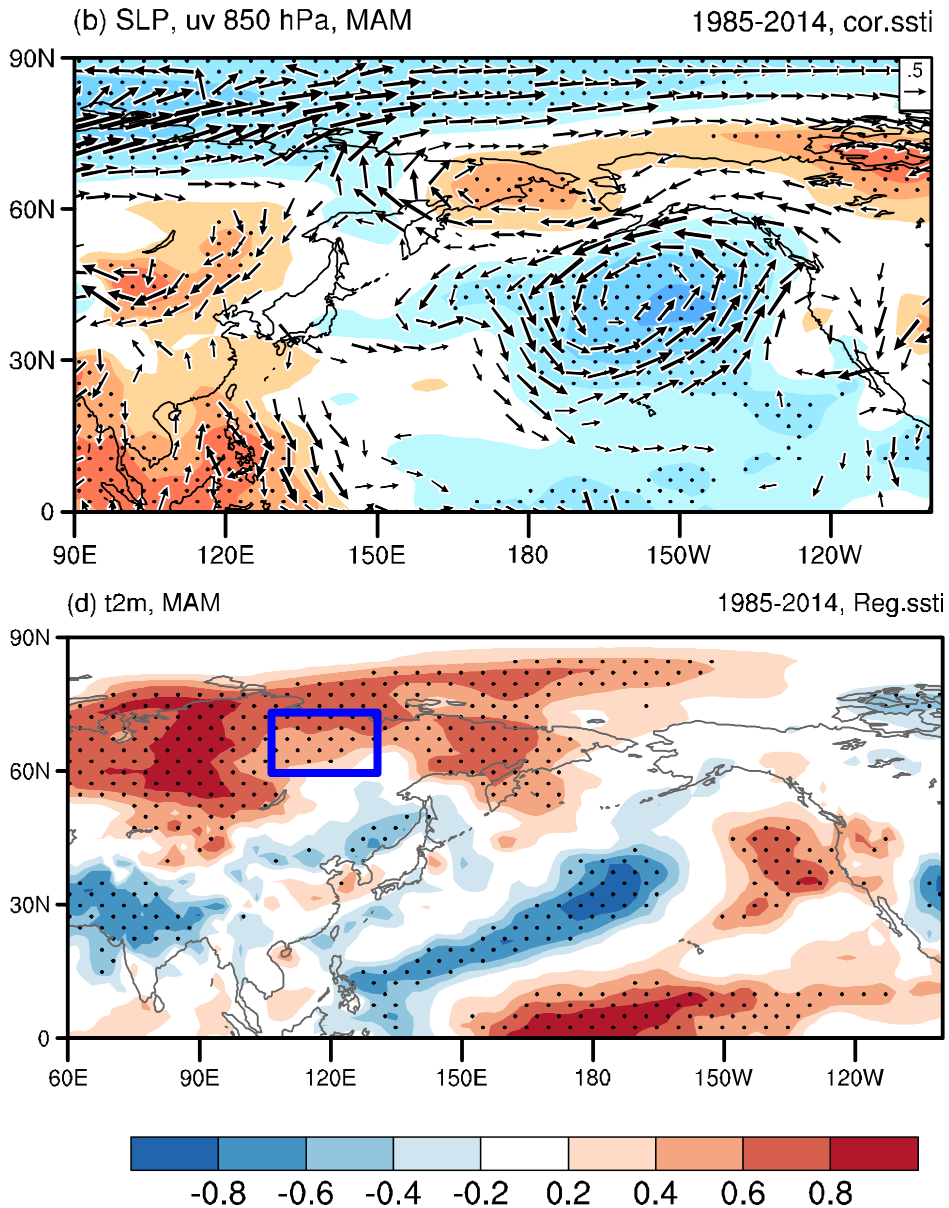

snow cover

SON

DJF

MAM

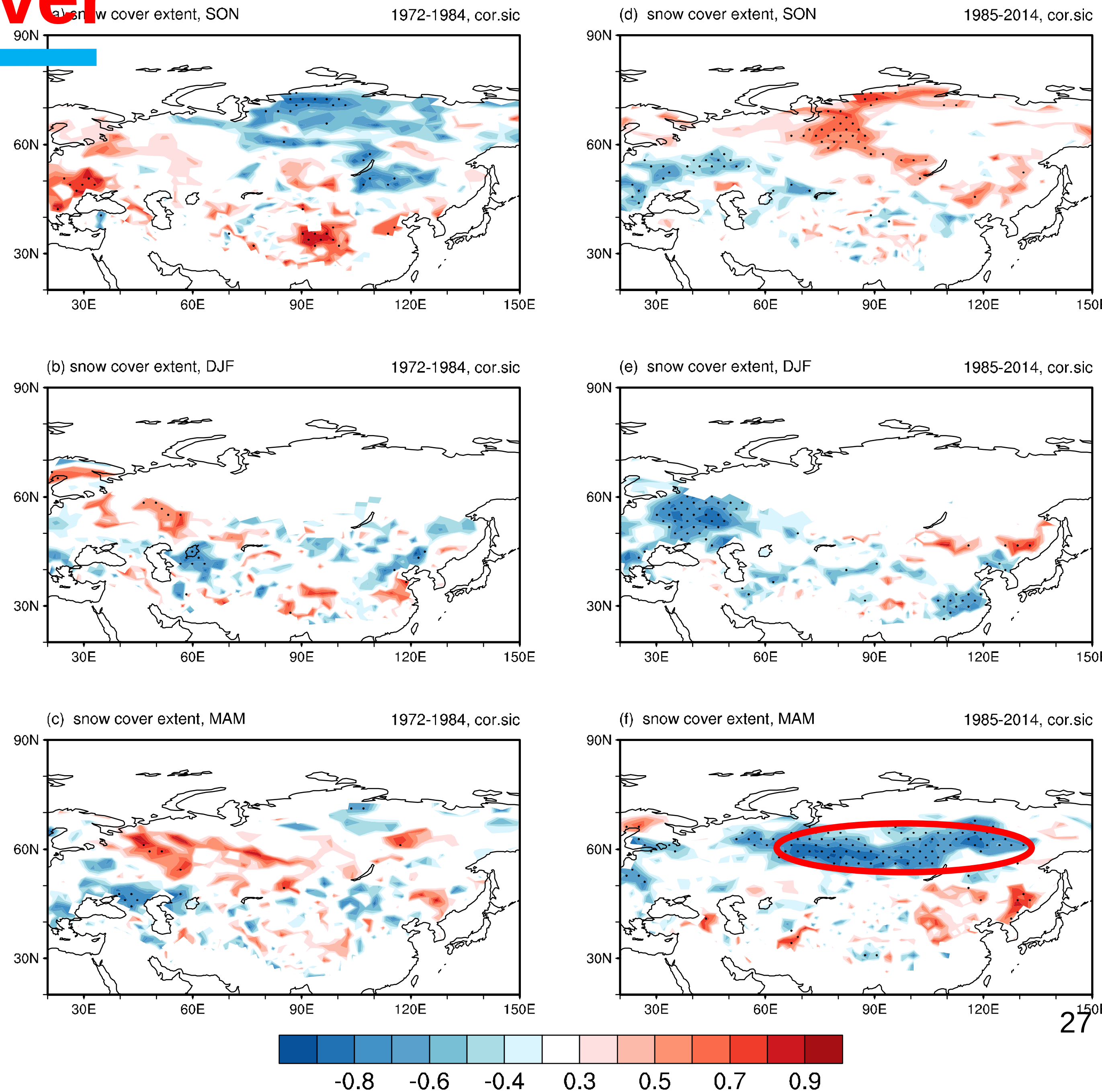

Summary

- The autumn Arctic sea ice (150ºE−150ºW, 70º−80ºN) is significantly related with the spring Eurasian soil moisture (60-70˚N, 110-130˚E) after the mid-1980s at interannual timescale.
- Positive anomalies of autumn Arctic sea ice → wave train pattern from the Arctic to Pacific → SST anomalies over the Pacific persist into spring → inducing higher temperature and less precipitation over Eurasia (60-70˚N, 110-130˚E) → lower soil moisture there

- **3. Simulation and Projection of Permafrost degradation on the Tibetan Plateau**

Method and data

HY data
(3 hourly, 0.1°×0.1°, Yang and He, 2010)

RegCM data
(6 hourly, 0.2°×0.2°, Gao et al., 2012)

CLM4.0
(Freeze/thaw, Soil organic matter, Soil depth 50 m, Lawrence et al.,2008)

Simulation,1981-2010

Projection, 2010-2100

Validation

Permafrost Degradation

Hydrology effect

Validation: Simulation VS. Observation

Observation (Li,1996)

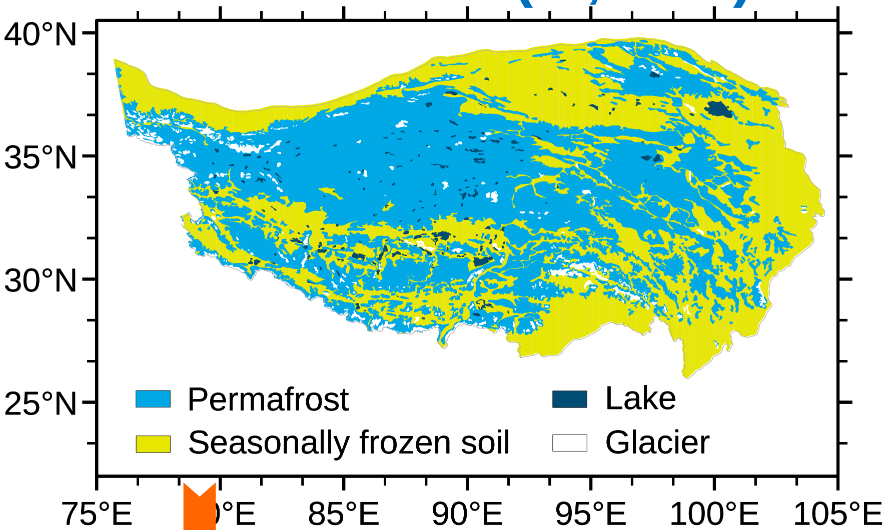

HY_Simulation (1981-2000)

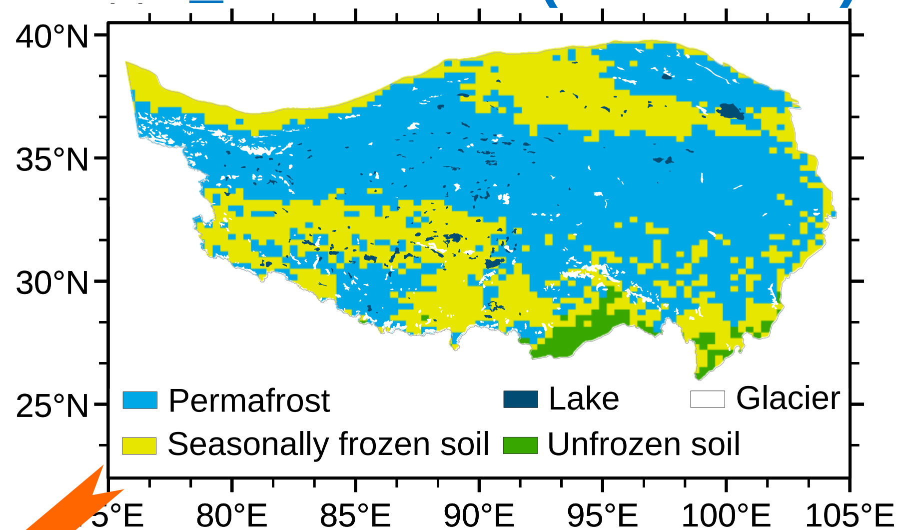

RegCM_Simulation (1981-2000)

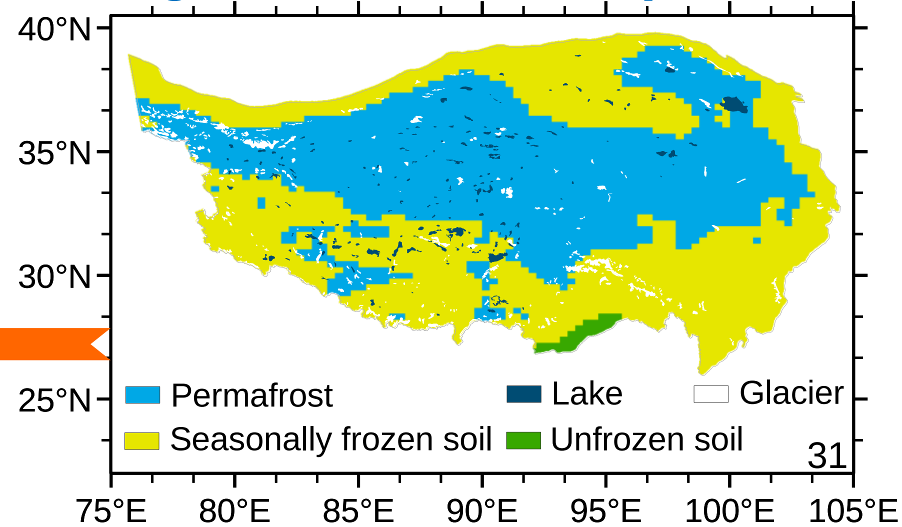

127×10^4 km^2

=

151×10^4 km^2

Permafrost Area = 122×10^4 km^2

Simulated Permafrost Change

2000s

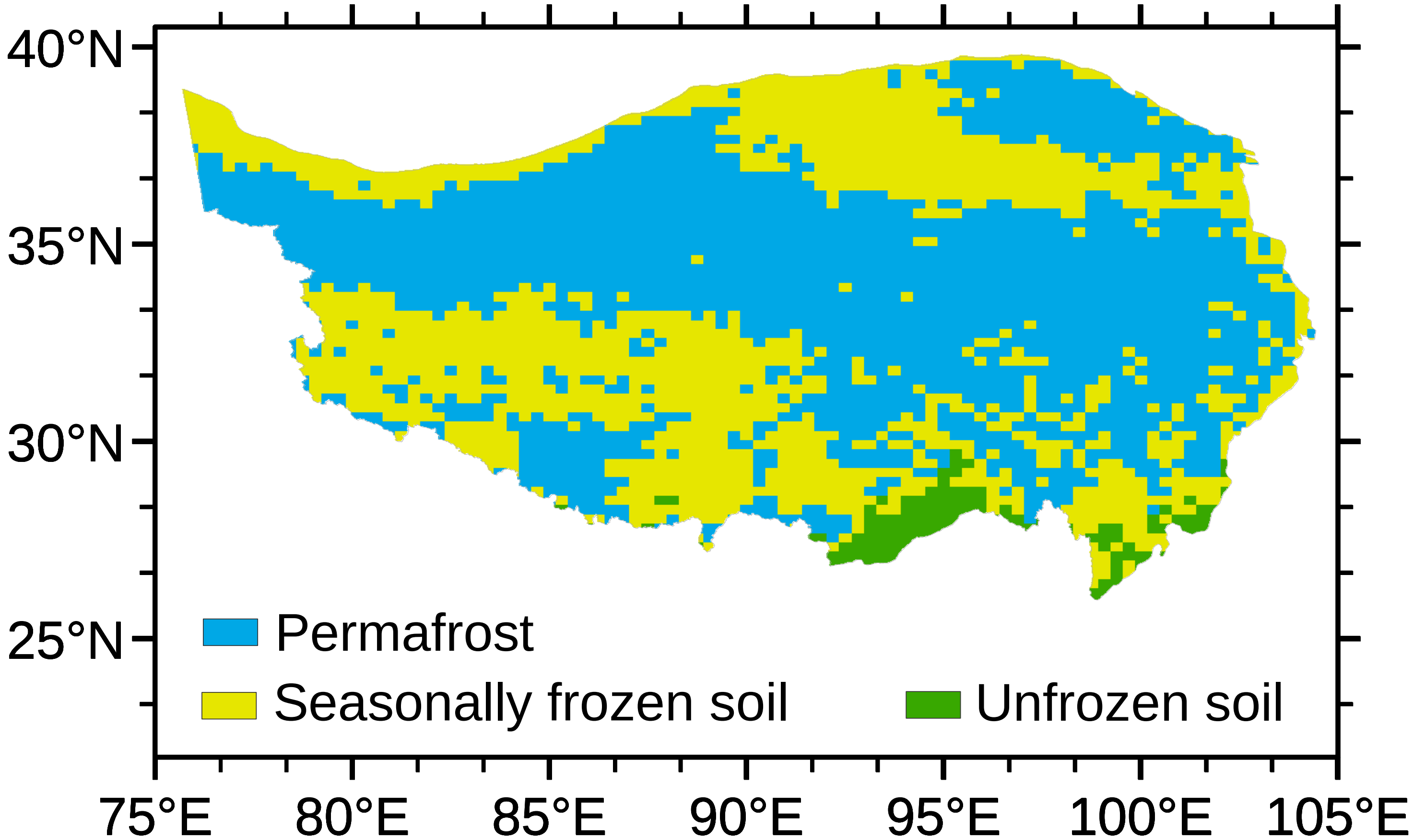

Area: 164,156,147 × 10^4 km^2 for 1980s,1990s,2000s,respectively

Simulated Series of Permafrost Area

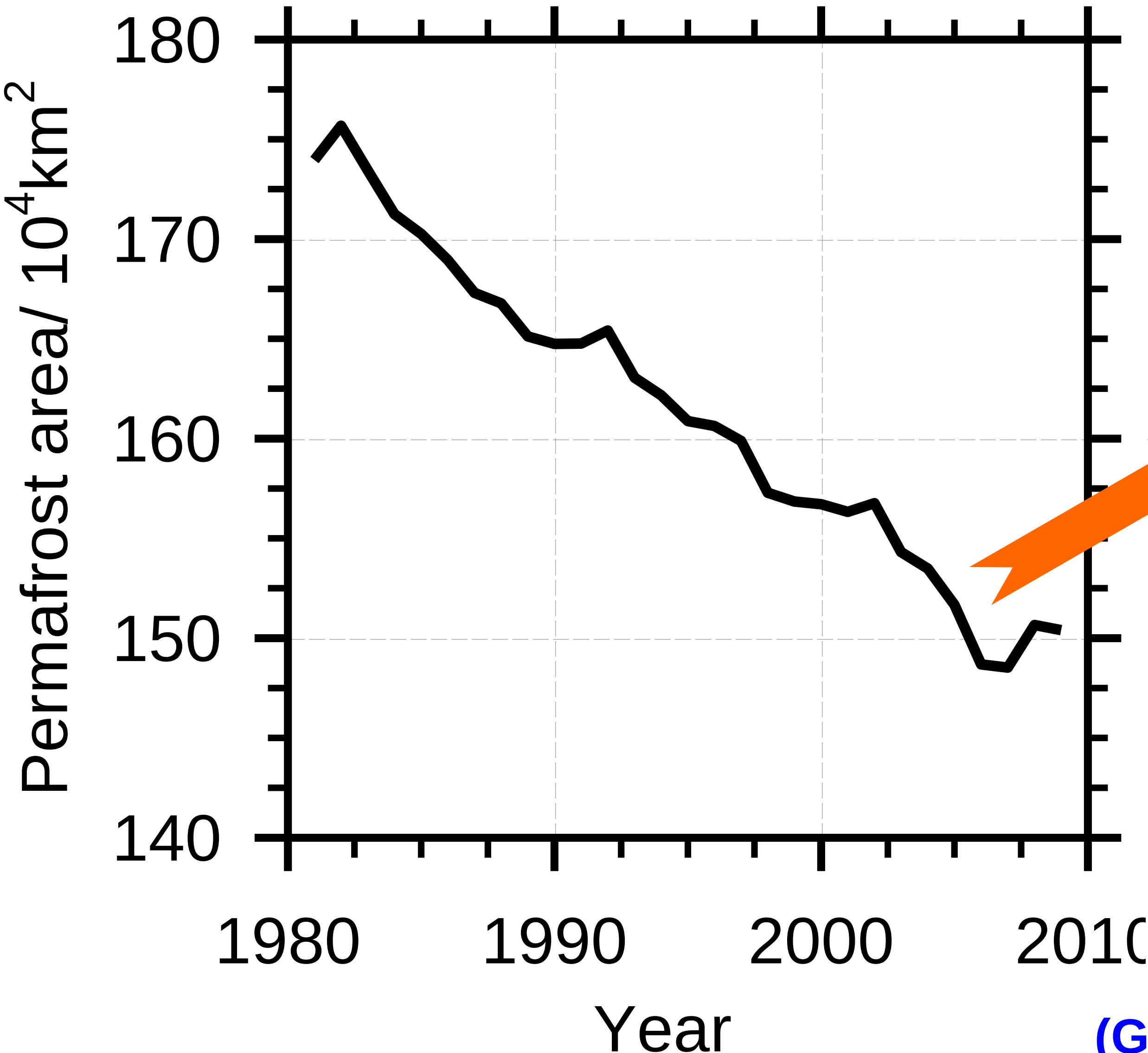

Decreasing rate: 9.2×10⁴ km²/decade

(Guo and Wang, 2013, *JGR*)

Projected Permafrost Degradation

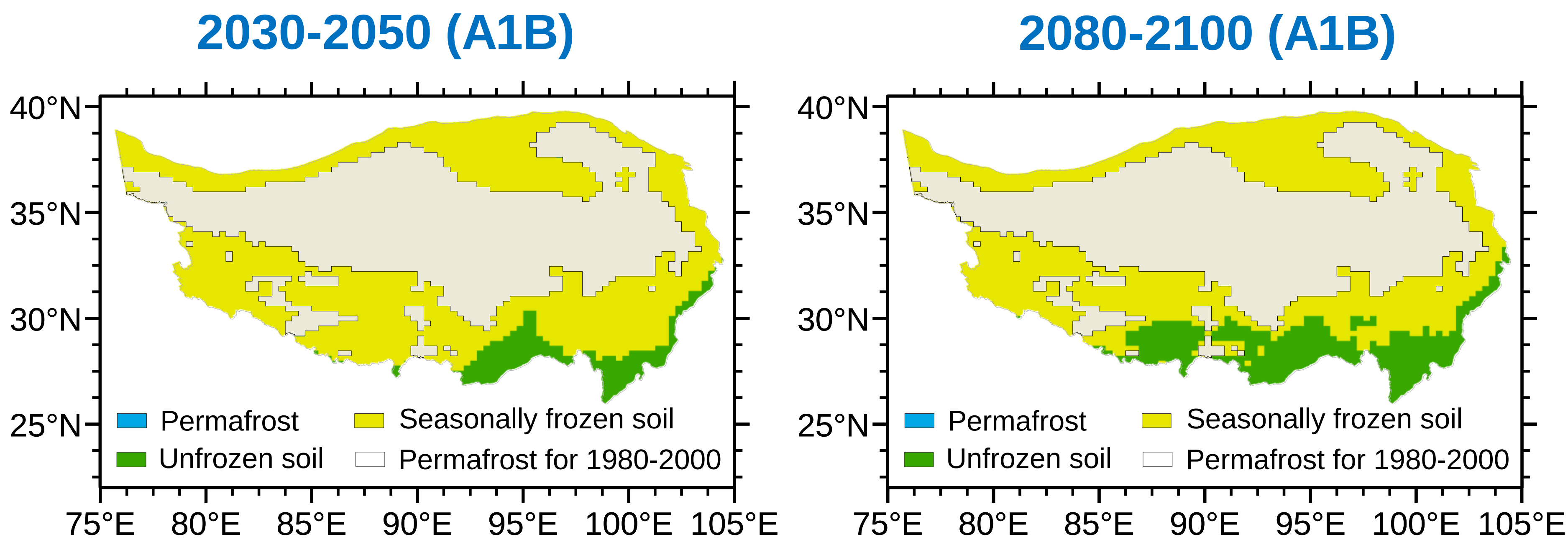

(Guo et al., 2012, *JGR*)

$\times 10^4$ km^2	1980-2000	2030-2050	2080-2100
Permafrost Area	**122.2**	**74.9 (*–39%*)**	**22.9 (*–81%*)**

Projected Series of Permafrost Area

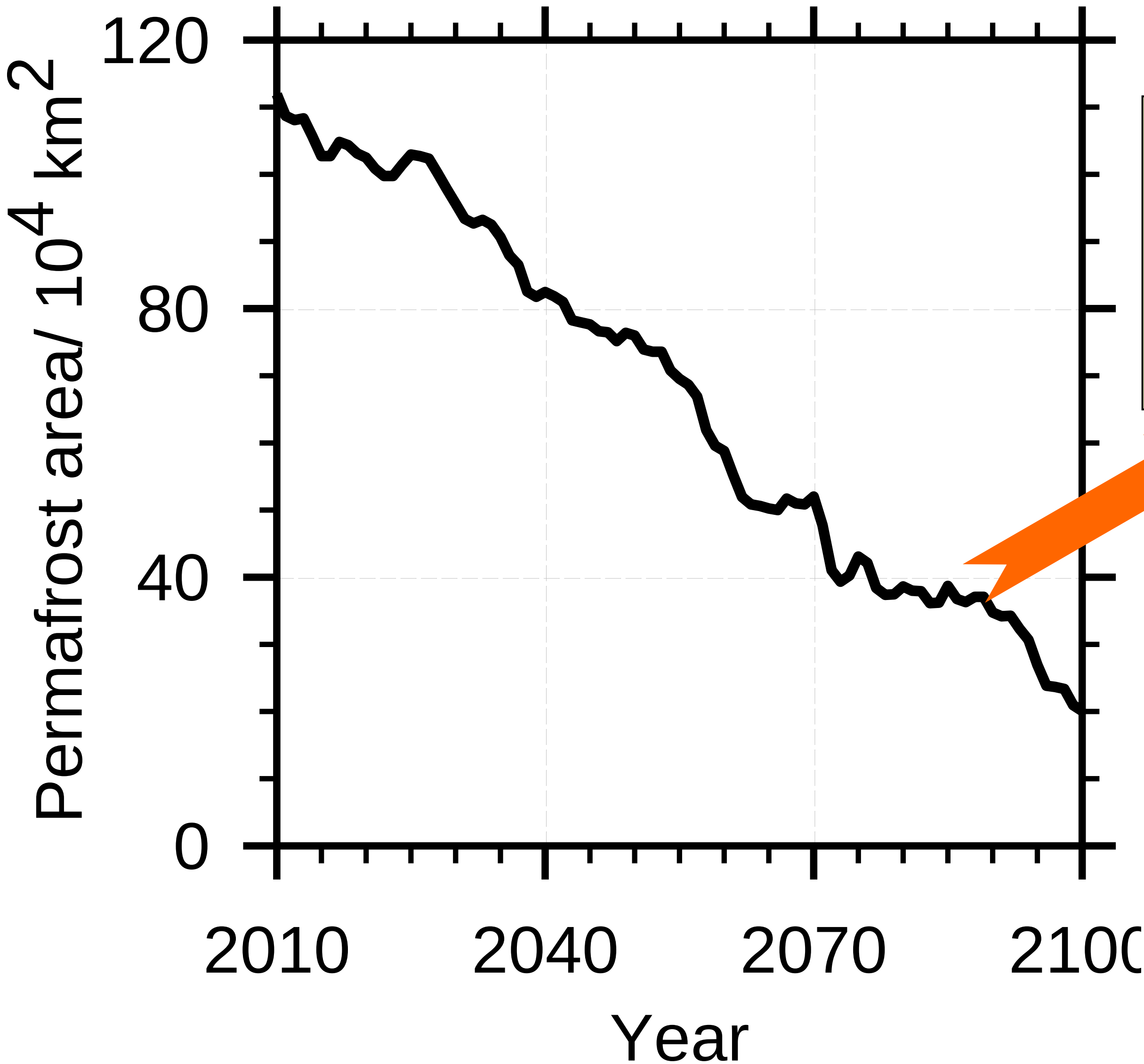

Decreasing rate: 10.4×10^4 km^2/decade

Summary

- Simulated present-day permafrost status was **reasonable**.
- Permafrost area decreased by **9.2×10^4 km^2/decade** during 1981-2010.
- Permafrost area would decrease by **39%** by the mid-21st century and by **81%** by the end of 21st century.
- Permafrost degradation could result in **reallocation** of total runoff.

Thank you for your attention.